

Hierarchy of the nonlocal advantage of quantum coherence and Bell nonlocality

Ming-Liang Hu,^{1,2,*} Xiao-Min Wang,¹ and Heng Fan^{2,3,4,†}

¹*School of Science, Xi'an University of Posts and Telecommunications, Xi'an 710121, China*

²*Institute of Physics, Chinese Academy of Sciences, Beijing 100190, China*

³*CAS Center for Excellence in Topological Quantum Computation, University of Chinese Academy of Sciences, Beijing 100190, China*

⁴*Songshan Lake Material Laboratory, Dongguan 523000, China*

Quantum coherence and nonlocality capture nature of quantumness from different aspects. For the two-qubit states with diagonal correlation matrix, we prove strictly a hierarchy between the nonlocal advantage of quantum coherence (NAQC) and Bell nonlocality by showing geometrically that the NAQC created on one qubit by local measurement on another qubit captures quantum correlation which is stronger than Bell nonlocality. For general states, our numerical results present strong evidence that this hierarchy may still hold. So the NAQC states form a subset of the states that can exhibit Bell nonlocality. We further propose a measure of NAQC that can be used for a quantitative study of it in bipartite states.

PACS numbers: 03.67.Mn, 03.65.Ta, 03.65.Yz

I. INTRODUCTION

Quantum correlations in states of composite systems can be characterized from different perspectives. From the applicative point of view, they are also invaluable physical resources which are recognized to be responsible for the power of those classically impossible tasks involving quantum communication and quantum computation [1]. Stimulated by this realization, there are a number of quantum correlation measures being put forward up to date [2–5]. Some of the extensively studied measures include Bell nonlocality (BN) [2], quantum entanglement [3], Einstein-Podolski-Rosen steering [4], and quantum discord [5]. For two-qubit states, a hierarchy of these quantum correlations has also been identified [6–11]. This hierarchy reveals different yet interlinked subtle nature of correlations, and broadens our understanding about the physical essence of quantumness in a state.

Quantum coherence is another basic notion in quantum theory, and recent years have witnessed an increasing interest on pursuing its quantification [12, 13]. In particular, based on a seminal framework formulated by Baumgratz *et al.* [14], there are various coherence measures being proposed [15–21]. This stimulates one's enthusiasm to understand them from different aspects, as for instance the distillation of coherence [19, 22], the role of coherence played in quantum state merging [23], and the characteristics of coherence under local quantum operations [24–27] and noisy quantum channels [28, 29]. Moreover, some fundamental aspects of coherence such as its role in revealing the wave nature of a system [30, 31], its tradeoffs under the mutually unbiased bases [32] or incompatible bases [33], have also been extensively studied.

Conceptually, coherence is thought to be more fundamental than various forms of quantum correlations, hence it is natural to pursue their interrelations for bipartite and multipartite systems. In fact, it has already been shown that coherence it-

self can be quantified by the entanglement created between the considered system and an incoherent ancilla [34]. There are also several works which linked coherence to quantum discord [35–37] and measurement-induced disturbance [38].

In a recent work, Mondal *et al.* [39] explored the interrelation of quantum coherence and quantum correlations from an operational perspective. By performing local measurements on qubit A of a two-qubit state AB , they showed that the average coherence of the conditional states of B summing over the mutually unbiased bases can exceed a threshold that cannot be exceeded by any single-qubit state. They termed this as the nonlocal advantage of quantum coherence (NAQC), and proved that any two-qubit state that can achieve a NAQC (we will call it the NAQC state for short) is quantum entangled. As there are many other quantum correlation measures, it is significant to pursue their connections with NAQC. We explore such a problem in this paper. For two-qubit states with diagonal correlation matrix, we showed strictly that quantum correlation responsible for NAQC is stronger than that responsible for BN, while for general states this result is conjectured based on numerical analysis. We hope this finding may shed some light on our current quest for a deep understanding of the interrelation between quantum coherence and quantum correlations in composite systems.

II. TECHNICAL PRELIMINARIES

We start by recalling two well-established coherence measures known as the l_1 norm of coherence and relative entropy of coherence [14]. For a state described by density operator ρ in the reference basis $\{|i\rangle\}$, they are given, respectively, by

$$C_{l_1}(\rho) = \sum_{i \neq j} |\langle i|\rho|j\rangle|, \quad C_{re}(\rho) = S(\rho_{\text{diag}}) - S(\rho), \quad (1)$$

where $S(\cdot)$ denotes the von Neumann entropy, and ρ_{diag} is an operator comprised of the diagonal part of ρ .

Using the above measures, Mondal *et al.* presented a “steering game” in Ref. [39]: Two players, Alice and Bob, share a

*Electronic address: mingliang0301@163.com

†Electronic address: hfan@iphy.ac.cn

two-qubit state ρ . They begin this game by agreeing on three observables $\{\sigma_1, \sigma_2, \sigma_3\}$, with $\sigma_{1,2,3}$ being the usual Pauli operators. Alice then measures qubit A and informs Bob of her choice σ_i and outcome $a \in \{0, 1\}$. Finally, Bob measures coherence of qubit B in the eigenbasis of either σ_j or σ_k ($j, k \neq i$) randomly. By denoting the ensemble of his conditional states as $\{p(a|\sigma_i), \rho_{B|\sigma_i^a}\}$, the average coherence is given by

$$\bar{C}_\alpha^{\sigma_j}(\{p(a|\sigma_i), \rho_{B|\sigma_i^a}\}) = \sum_a p(a|\sigma_i) C_\alpha^{\sigma_j}(\rho_{B|\sigma_i^a}), \quad (2)$$

where $p(a|\sigma_i) = \text{tr}(\Pi_i^a \rho)$, $\rho_{B|\sigma_i^a} = \text{tr}_A(\Pi_i^a \rho) / p(a|\sigma_i)$, $\Pi_i^a = [I_2 + (-1)^a \sigma_i] / 2$, I_2 is the identity operator, and $C_\alpha^{\sigma_j}$ ($\alpha = l_1$ or re) is the coherence defined in the eigenbasis of σ_j .

By further averaging over the three possible measurements of Alice and the corresponding possible reference eigenbases chosen by Bob, Mondal *et al.* [39] derived the criterion for achieving NAQC, which is given by

$$C_\alpha^{na}(\rho) = \frac{1}{2} \sum_{\substack{i,j,a \\ i \neq j}} p(a|\sigma_i) C_\alpha^{\sigma_j}(\rho_{B|\sigma_i^a}) > C_\alpha^m, \quad (3)$$

where $C_{l_1}^m = \sqrt{6}$, $C_{re}^m = 3H(1/2 + \sqrt{3}/6) \simeq 2.2320$, and $H(\cdot)$ stands for the binary Shannon entropy function.

In fact, the above critical values are also direct results of the complementarity relations of coherence under mutually unbiased bases [32]. To be explicit, by Eq. (4) of Ref. [32] and the mean inequality (the arithmetic mean of a list of nonnegative real numbers is not larger than the quadratic mean of the same list) one can obtain the critical value $C_{l_1}^m$, while from Eq. (24) of Ref. [32] one can obtain the critical value C_{re}^m .

To detect nonlocality in ρ , one can use the Bell-CHSH inequality $|\langle B_{\text{CHSH}} \rangle_\rho| \leq 2$, where B_{CHSH} is the Bell operator [40]. Violation of this inequality implies that ρ is Bell nonlocal. The maximum of $|\langle B_{\text{CHSH}} \rangle_\rho|$ over all mutually orthogonal pairs of unit vectors in \mathbb{R}^3 is given by [41]

$$B_{\text{max}}(\rho) = 2 \sqrt{M(\rho)}, \quad (4)$$

where $M(\rho) = u_1 + u_2$, with u_i ($i = 1, 2, 3$) being the eigenvalues of $T^\dagger T$ arranged in nonincreasing order, and T stands for the matrix formed by elements $t_{ij} = \text{tr}(\rho \sigma_i \otimes \sigma_j)$. Clearly, $M(\rho) > 1$ is also a manifestation of BN in ρ .

It has been shown that any ρ that can achieve a NAQC is entangled, while the opposite case is not always true [39]. This gives rise to a hierarchy of them. To further establish the hierarchy between NAQC and BN, and based on the consideration that the BN is local unitary invariant, we first consider the representative class of two-qubit states

$$\tilde{\rho} = \frac{1}{4} (I_4 + \vec{r} \cdot \vec{\sigma} \otimes I_2 + I_2 \otimes \vec{s} \cdot \vec{\sigma} + \sum_{i=1}^3 v_i \sigma_i \otimes \sigma_i), \quad (5)$$

where $\{\vec{r}, \vec{s}, \vec{v}\} \in \mathbb{R}^3$ satisfy the physical requirement $\tilde{\rho} \geq 0$. For $\vec{r} = \vec{s} = \vec{0}$, it reduces to the Bell-diagonal state ρ_{Bell} which is characterized by the tetrahedron \mathcal{T} [see Fig. 1(a)], and the region of separable ρ_{Bell} is the octahedron \mathcal{O} [42]. For $\vec{r} \cdot \vec{s} \neq 0$, physical $\tilde{\rho}$ shrinks to partial regions of \mathcal{T} . For this case, while the separable region is still inside \mathcal{O} , the entangled ones may not be limited to the four regions outside \mathcal{O} .

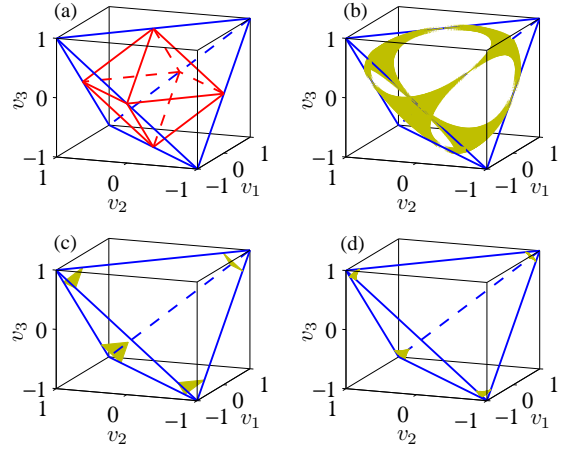


FIG. 1: The tetrahedron \mathcal{T} and octahedron \mathcal{O} associated with ρ_{Bell} (a), and the level surfaces of $M(\tilde{\rho}) = 1$ (b), $C_{l_1}^{na}(\rho_{\text{Bell}}) = \sqrt{6}$ (c), and $C_{re}^{na}(\rho_{\text{Bell}}) = C_{re}^m$ (d). The regions of Bell nonlocal states $\tilde{\rho}$ and NAQC states ρ_{Bell} are those outside the level surfaces.

III. HIERARCHY OF NAQC AND BN

The hierarchy of entanglement, steering, and BN shows that while entanglement clearly reveals the nonclassical nature of a state, steering and BN exhibit even stronger deviations from classicality [6–11]. Here, we show that NAQC may be viewed as a quantum correlation which is even stronger than BN.

To begin with, we prove the convexity of NAQC,

$$C_\alpha^{na} \left(\sum_k q_k \rho_k \right) \leq \sum_k q_k C_\alpha^{na}(\rho_k), \quad (6)$$

that is, the NAQC is nonincreasing under mixing of states. By combining Eqs. (2) and (3), one can see that the NAQC is convex provided $\bar{C}_\alpha^{\sigma_j}$ is convex. For $\rho = \sum_k q_k \rho_k$, the conditional state of B after Alice's local measurements is

$$\rho_{B|\sigma_i^a} = \frac{\sum_k q_k \text{tr}_A(\Pi_i^a \rho_k)}{\sum_k q_k \text{tr}(\Pi_i^a \rho_k)} = \frac{\sum_k q_k p_k(a|\sigma_i) \rho_{B|\sigma_i^a}^k}{p(a|\sigma_i)}, \quad (7)$$

where $\rho_{B|\sigma_i^a}^k = \text{tr}_A(\Pi_i^a \rho_k) / p_k(a|\sigma_i)$, $p_k(a|\sigma_i) = \text{tr}(\Pi_i^a \rho_k)$, and we have denoted by $p(a|\sigma_i) = \sum_k q_k p_k(a|\sigma_i)$. Then

$$\begin{aligned} \bar{C}_\alpha^{\sigma_j}(\{p(a|\sigma_i), \rho_{B|\sigma_i^a}\}) &= \sum_a p(a|\sigma_i) C_\alpha^{\sigma_j}(\rho_{B|\sigma_i^a}) \\ &\leq \sum_{k,a} p(a|\sigma_i) \frac{q_k p_k(a|\sigma_i)}{p(a|\sigma_i)} C_\alpha^{\sigma_j}(\rho_{B|\sigma_i^a}^k) \\ &= \sum_{k,a} q_k p_k(a|\sigma_i) C_\alpha^{\sigma_j}(\rho_{B|\sigma_i^a}^k) \\ &= \sum_k q_k \bar{C}_\alpha^{\sigma_j}(\{p_k(a|\sigma_i), \rho_{B|\sigma_i^a}^k\}), \end{aligned} \quad (8)$$

where the first inequality is due to convexity of the coherence measure. This completes the proof of Eq. (6).

Next, we give the level surface \mathcal{S} of constant BN $M(\tilde{\rho}) = 1$. It can be divided into four parts, corresponding to the four vertices of \mathcal{T} . For convenience of later presentation, we denote

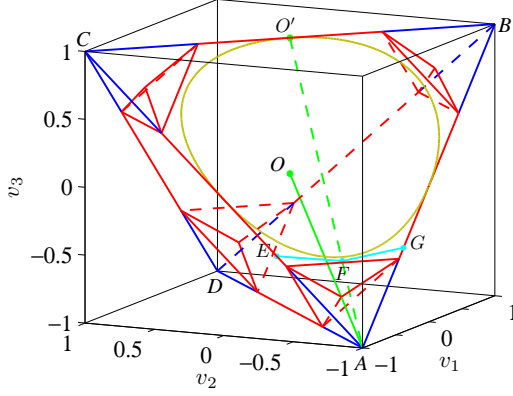


FIG. 2: Geometric representation of the polyhedron \mathcal{P} (the red lines) inside \mathcal{T} . Here, O and O' are the coordinate origin and the midpoint of BC , respectively, while the khaki curve is the curve of constant BN $M(\tilde{\rho}) = 1$ at the facet ABC .

by \mathcal{S}_A the part near vertex A (see Fig. 2). It is described by

$$\begin{aligned} v_i &= \sin \theta, \quad v_j = \cos \theta, \\ v_k &\in [\max\{\sin \theta, \cos \theta\}, 1 + \sin \theta + \cos \theta], \quad \theta \in [\pi, 1.5\pi], \end{aligned} \quad (9)$$

where $(i, j, k) = (1, 2, 3), (2, 3, 1),$ and $(3, 1, 2)$. The equations for the other three parts of \mathcal{S} can be obtained directly by their symmetry about the coordinate origin O . The corresponding results are showed in Fig. 1(b).

In the following, we denote by \mathcal{N} the set of NAQC states and \mathcal{B} the set of Bell nonlocal states. We will prove the inclusion relation $\mathcal{N} \subset \mathcal{B}$ for any $\tilde{\rho}$, meaning that the existence of NAQC implies the existence of BN.

A. l_1 norm of NAQC

First, we consider the class of Bell-diagonal states. Without loss of generality, we assume $|v_1| \geq |v_2| \geq |v_3|$, then

$$C_{l_1}^{na}(\rho_{\text{Bell}}) = \sum_i |v_i|, \quad M(\rho_{\text{Bell}}) = v_1^2 + v_2^2, \quad (10)$$

from which one can obtain $|v_1| > \sqrt{6}/3$ and $|v_2| > (\sqrt{6} - 1)/2$ when $C_{l_1}^{na}(\rho_{\text{Bell}}) > \sqrt{6}$. This further gives rise to $M(\rho_{\text{Bell}}) > 1$. That is, any ρ_{Bell} that can achieve a NAQC is Bell nonlocal. But the converse is not true, e.g., if $v_{1,2,3} \in [-\sqrt{6}/3, -1/\sqrt{2}]$, we have $M(\rho_{\text{Bell}}) > 1$ and $C_{l_1}^{na}(\rho_{\text{Bell}}) \leq \sqrt{6}$. With all this, we arrived at the inclusion relation $\mathcal{N} \subset \mathcal{B}$. The level surfaces of $C_{l_1}^{na}(\rho_{\text{Bell}}) = \sqrt{6}$ can be found in Fig. 1(c).

Second, we consider $\tilde{\rho}$ sitting at the edges of \mathcal{T} with general \vec{r} and \vec{s} . We take the edge AB as an example (see Fig. 2), the cases for the other edges are similar. Along this edge, we have $v_1 = v_3$ and $v_2 = -1$, then one can determine analytically the constraints imposed by $\tilde{\rho} \geq 0$ on the involved parameters as $r_{1,3} = s_{1,3} = 0$, $r_2 = -s_2$, and $s_2^2 \leq 1 - v_1^2$ (see Appendix A). Thus we have

$$C_{l_1}^{na}(\tilde{\rho}) = 1 + |v_1| + \sqrt{v_1^2 + s_2^2}. \quad (11)$$

It is always not larger than $\sqrt{6}$ in the region of $|v_1| \leq \sqrt{6} - 2$. On the other hand, the states located at the edge AB other than its midpoint are Bell nonlocal. Hence, the inclusion relation $\mathcal{N} \subset \mathcal{B}$ holds for all $\tilde{\rho}$ located at the edges of \mathcal{T} .

Next, we consider $\tilde{\rho}$ associated with $v_{1,2,3} = v_0 = -1/\sqrt{2}$. As $C_{l_1}^{na}$ is an increasing function of $|s_i|$ ($i = 1, 2, 3$), one only needs to determine the maximal $|s_i|$ for which $\tilde{\rho} \geq 0$. Without loss of generality, we assume $s_3 = w_0 s_1$ and $s_2 = w_1 s_1$, then a detailed analysis shows that the resulting maximum NAQC states belong to the set of $\tilde{\rho}$ with $r_3 = w_0 r_1$ and $r_2 = w_1 r_1$. Under this condition, one can obtain analytically the eigenvalues ϵ_k of $\tilde{\rho}$. Then from $\epsilon_k \geq 0$ ($\forall k$) one can obtain

$$\begin{aligned} |s_1 + r_1| \leq c_1 &= \frac{1 + v_0}{\sqrt{1 + w_0^2 + w_1^2}}, \\ |s_1 - r_1| \leq c_2 &= \sqrt{\frac{1 - 2v_0 - 3v_0^2}{1 + w_0^2 + w_1^2}}. \end{aligned} \quad (12)$$

For state $\tilde{\rho}$ with fixed v_0, w_0 , and w_1 , $C_{l_1}^{na}$ takes its maximum when the above inequalities become equalities. That is, when

$$s_1 = \pm \frac{1}{2}(c_1 + c_2), \quad r_1 = \pm \frac{1}{2}(c_1 - c_2), \quad (13)$$

then by further maximizing the resulting $C_{l_1}^{na}$ over w_0 and w_1 , we obtain $C_{l_1, \text{max}}^{na} \approx 2.4405$ at the critical points $w_{0,1} = \pm 1$ (we have also checked the validity of this result with 10^7 randomly generated $\tilde{\rho}$ for which $v_{1,2,3} = -1/\sqrt{2}$, and no violation was observed). As this maximum is smaller than $\sqrt{6}$, any $\tilde{\rho}$ with $v_0 = -1/\sqrt{2}$ cannot achieve a NAQC.

To proceed, we introduce a polyhedron \mathcal{P} with the set of its vertices near the vertex A being given by $(v_0, v_0, v_0), (-1, \gamma, \gamma), (\gamma, -1, \gamma), (\gamma, \gamma, -1)$, and its other vertices can be obtained by using their symmetry with respect to the point O (see Fig. 2). One can show that when $|\gamma| < \sqrt{2} - 1$, the surface \mathcal{S}_A is always inside \mathcal{P} (see Appendix B). Finally, as $C_{l_1, \text{max}}^{na} \approx 2.4405$ at the point (v_0, v_0, v_0) , we choose $\gamma = 2 - \sqrt{6}$ for which $C_{l_1}^{na}$ is also smaller than $\sqrt{6}$ at the other three points of \mathcal{P} near vertex A [see Eq.(11)], then as any physical state with \vec{v} inside \mathcal{P} can be written as a convex combination of states with \vec{v} at the vertices of \mathcal{P} , we complete the proof of the inclusion relation $\mathcal{N} \subset \mathcal{B}$ for general $\tilde{\rho}$ by using the convexity of NAQC.

In fact, for $\tilde{\rho}$ at the line AO with fixed w_0 and w_1 , one can obtain the critical v_0^c at which $C_{l_1}^{na} = \sqrt{6}$. As $C_{l_1}^{na}$ and v_0^c considered here are invariant under the substitution $w_0 \leftrightarrow w_1$, we showed in Fig. 3(a) an exemplified plot of the w_0 dependence of v_0^c with fixed $w_1 = 0$ and 1. It first increases to a peak value at $w_0 = 1$, then decreases gradually with the increase of $|\omega_0|$. By optimizing over w_0 and w_1 , one can further obtain the region of $v_0^c \in (-0.7519, -0.7142)$, where the lower and upper bounds correspond to $w_{0,1} = 0$ and $w_{0,1} = \pm 1$, respectively. Clearly, the point (v_0^c, v_0^c, v_0^c) is always outside the surface \mathcal{S} .

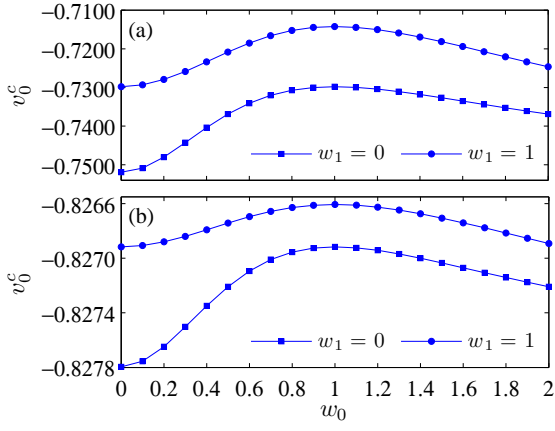


FIG. 3: Critical v_0^c for which (a) $C_{l_1}^{na} = \sqrt{6}$ and (b) $C_{re}^{na} = C_{re}^m$ versus w_0 with $w_1 = 0$ and 1. The other parameters are $\vec{s} = (s_1, w_0 s_1, w_1 s_1)$ and $\vec{r} = (r_1, w_0 r_1, w_1 r_1)$, with s_1 and r_1 being given in Eq. (13), and v_0^c is plotted in the region of $v_0 < 0$.

B. Relative entropy of NAQC

In this subsection, we consider NAQC measured by the relative entropy. First, for Bell-diagonal states, the corresponding NAQC can be obtained as [39]

$$C_{re}^{na}(\rho_{\text{Bell}}) = 3 - \sum_i H\left(\frac{1+v_i}{2}\right). \quad (14)$$

Then by imposing $C_{re}^{na}(\rho_{\text{Bell}}) > C_{re}^m$ with the assumption $|v_1| \geq |v_2| \geq |v_3|$, one can obtain

$$H\left(\frac{1+v_1}{2}\right) < \frac{3-C_{re}^m}{3}, \quad H\left(\frac{1+v_2}{2}\right) < \frac{3-C_{re}^m}{2}, \quad (15)$$

which yields $M(\rho_{\text{Bell}}) > 1$. Moreover, we have $M(\rho_{\text{Bell}}) > 1$ and $C_{re}^{na}(\rho_{\text{Bell}}) < C_{re}^m$ for $v_{1,2,3} \in (-0.9140, -1/\sqrt{2})$. So $\mathcal{N} \subset \mathcal{B}$ holds for ρ_{Bell} . The corresponding level surfaces were showed in Fig. 1(d). Clearly, the region of NAQC states shrinks with that captured by the l_1 norm.

For $\tilde{\rho}$ sitting at the edges of \mathcal{T} with general \vec{r} and \vec{s} , we take the edge AB as an example. Based on the results of Sec. III A, one can obtain

$$C_{re}^{na} = 2 + H\left(\frac{1+s_2}{2}\right) - 2H\left(\frac{1+\sqrt{v_1^2+s_2^2}}{2}\right), \quad (16)$$

then it is direct to show that C_{re}^{na} is always smaller than C_{re}^m for $|v_1| < -b_0 \approx 0.3813$. So the inclusion relation $\mathcal{N} \subset \mathcal{B}$ holds for any $\tilde{\rho}$ at the edges of \mathcal{T} .

Based on the above preliminaries, we now consider $\tilde{\rho}$ at the surface \mathcal{S}_A (the cases for the other parts of \mathcal{S} are similar). We will show that for these $\tilde{\rho}$ the inequality $C_{re}^{na} < C_{re}^m$ holds. Then by further employing the convexity of NAQC and the fact that $\{\tilde{\rho}\}$ is a convex set, one can complete the proof of $\mathcal{N} \subset \mathcal{B}$. In fact, due to the structure of \mathcal{S}_A [see Eq. (9)], it suffices to prove that we always have $C_{re}^{na} < C_{re}^m$ at the boundary of \mathcal{S}_A .

First, we introduce the polygon line EFG over $(-1, b_0, b_0)$, $(a_0, a_0, 1+2a_0)$, and $(b_0, -1, b_0)$. One can prove that there is no intersection of this line and the boundary of \mathcal{S}_A at the facet ABC when $a_0 \lesssim -0.7082$ (Appendix B). Moreover, along the line AO' , $\tilde{\rho} \geq 0$ yields $r_{1,2} = -s_{1,2}$ and $r_3 = s_3$ (Appendix A), then one can obtain that at the point F with $a_0 = -0.7082$, C_{re}^{na} maximized over \vec{r} and \vec{s} is of about 1.4956. As C_{re}^{na} is also smaller than C_{re}^m at the points E and G [see Eq. (16)], we have $C_{re}^{na} < C_{re}^m$ for any $\tilde{\rho}$ at this boundary.

Second, if we make the substitutions $v_0 = -0.7082$ and $\gamma = b_0$ to the vertices of \mathcal{P} , then one can show that the boundary of \mathcal{S}_A inside \mathcal{T} is also inside \mathcal{P} (see Appendix B). For $\tilde{\rho}$ at the point (v_0, v_0, v_0) , our numerical results showed that with fixed v_0 , w_0 , and w_1 , C_{re}^{na} also takes its maximum when s_1 and r_1 are given by Eq. (13). Then by further maximizing it over w_0 and w_1 , we obtain $C_{re, \text{max}}^{na} \approx 2.0041$ at $w_{0,1} = \pm 1$. As C_{re}^{na} is also smaller than C_{re}^m for $\tilde{\rho}$ at the vertices of \mathcal{P} with $\gamma = b_0$ [see Eq. (16)], we have $C_{re}^{na} < C_{re}^m$ for any $\tilde{\rho}$ at this boundary.

Similar to the l_1 norm of NAQC, one can obtain v_0^c at which $C_{re}^{na} = C_{re}^m$ with fixed w_0 and w_1 . It is $v_0^c \in (-0.8278, -0.8266)$, where the lower and upper bounds are obtained with $w_{0,1} = 0$ and $w_{0,1} = \pm 1$, respectively. As is showed in Fig. 3, v_0^c for the two NAQCs exhibits qualitatively the same w_0 dependence.

Before ending this section, we would like to mention here that although for the set of Bell-diagonal states, one detects a wider region of NAQC states by using the l_1 norm as a measure of coherence than that by using the relative entropy (see Fig. 1), this is not always the case. A typical example is that for $\tilde{\rho}$ at the edge AB of \mathcal{T} with $|v_{1,3}| \in (0.3813, \sqrt{6}-2)$, one may have $C_{l_1}^{na} < \sqrt{6}$ and $C_{re}^{na} > C_{re}^m$.

IV. AN EXPLICIT APPLICATION OF NAQC

As it is a proven fact that all Bell nonlocal states are useful for quantum teleportation [43], the hierarchy we obtained implies that any NAQC state $\tilde{\rho}$ can serve as a quantum channel for quantum teleportation. That is, it always gives rise to the average fidelity $F_{av} > 2/3$. In fact, F_{av} achievable with the channel state $\tilde{\rho}$ is given by [43]

$$F_{av}(\tilde{\rho}) = \frac{1}{2} + \frac{1}{6} \sum_i |v_i|. \quad (17)$$

Using this equation and the results of Sec. III, one can obtain that for any NAQC state $\tilde{\rho}$ captured by $C_{l_1}^{na}(\tilde{\rho})$, we always have $F_{av} > \sqrt{6}/3$, while for any NAQC state $\tilde{\rho}$ captured by $C_{re}^{na}(\tilde{\rho})$, we always have $F_{av} \geq 0.7938$. Both the two critical values are larger than $2/3$, so any NAQC state $\tilde{\rho}$ can serve as a quantum channel for nonclassical teleportation.

If we focus only on the class of NAQC Bell-diagonal states, the average fidelity F_{av} can be further improved. More specifically, Eqs. (10) and (14) imply that $F_{av} > (3 + \sqrt{6})/6$ for any NAQC state ρ_{Bell} captured by $C_{l_1}^{na}(\rho_{\text{Bell}})$, and $F_{av} \geq 0.9501$ for any NAQC state ρ_{Bell} captured by $C_{re}^{na}(\rho_{\text{Bell}})$.

V. SUMMARY AND DISCUSSION

In summary, we have explored the interrelations of NAQC achievable in a two-qubit state under local measurements and BN detected by violation of the Bell-CHSH inequality. There are two different scenarios of NAQC being considered: one is characterized by the l_1 norm of coherence, and another one is characterized by the relative entropy of coherence. For both scenarios, we showed geometrically that the inclusion relation $\mathcal{N} \subset \mathcal{B}$ holds for the class of states $\tilde{\rho}$ that have diagonal correlation matrix T . This extends the known hierarchy in quantum correlation, viz., BN, steerability, entanglement, and quantum discord to include NAQC.

One may also concern whether the obtained hierarchy holds for ρ with nondiagonal T . As such ρ is locally unitary equivalent to $\tilde{\rho}$, that is, $\rho = U_{AB}\tilde{\rho}U_{AB}^\dagger$ with $U_{AB} = U_A \otimes U_B$, the proof can be completed by showing that for any $\tilde{\rho}$ with $M(\tilde{\rho}) \leq 1$, we have $C_\alpha^{na}(U_{AB}\tilde{\rho}U_{AB}^\dagger) \leq C_\alpha^m$ for all unitaries U_{AB} . But due to the so many number of state parameters involved, it is difficult to give such a strict proof. For special cases, a strict proof may be available, e.g., for the locally unitary equivalent class of $\tilde{\rho}$ with $|\tilde{v}^2 + 2|\tilde{s}^2| \leq 2$, we are sure that $C_{l_1}^{na} \leq \sqrt{6}$, while for the locally unitary equivalent class of ρ_{Bell} , we are sure that $C_{re}^{na} \leq C_{re}^m$ (see Appendix C). Moreover, for $\tilde{\rho}$ with reduced number of parameters, we performed numerical calculations with 10^7 equally distributed local unitaries generated according to the Haar measure [44, 45], and found that C_α^{na} is always smaller than C_α^m (see Appendix C). These results presented strong evidence that the hierarchy may hold for any two-qubit state, though a strict proof is still needed.

Moreover, one may argue that NAQC can be recognized as a quantum correlation. It is stronger than BN in the sense that the NAQC states form a subset of the Bell nonlocal states. But it is asymmetric, that is, in general C_α^{na} defined with the local measurements on A does not equal that defined with the local measurements on B . This property is the same to steerability and quantum discord. The NAQC is also not locally unitary invariant. Its value may be changed by performing local unitary transformation to the mutually unbiased bases. To avoid this perplexity, one can define

$$\tilde{C}_\alpha^{na}(\rho) = \frac{1}{2} \max_{\{U_A \otimes U_B\}} \sum_{\substack{i,j,a \\ i \neq j}} p(a|\sigma_{i,U_A}) C_\alpha^{\sigma_{i,U_B}}(\rho_{B|\sigma_{i,U_A}}), \quad (18)$$

with $\sigma_{i,U_A} = U_A \sigma_i U_A^\dagger$, and likewise for σ_{j,U_B} . As BN is locally unitary invariant, we have $\tilde{\mathcal{N}} \subset \mathcal{B}$ provided $\mathcal{N} \subset \mathcal{B}$, where $\tilde{\mathcal{N}}$ is the set of NAQC states captured by $\tilde{C}_\alpha^{na}(\rho) > C_\alpha^m$.

Finally, in light of those measures of steerability based on the maximal violation of various steering inequalities and the similar measure of Bell nonlocality [9, 10], it is natural to quantify the degree of NAQC in a bipartite state ρ by

$$\tilde{Q}_\alpha(\rho) = \max \left\{ 0, \frac{\tilde{C}_\alpha^{na}(\rho) - C_\alpha^m}{\tilde{C}_{\alpha,\max}^{na} - C_\alpha^m} \right\}, \quad (19)$$

where $\tilde{C}_{\alpha,\max}^{na} = \max_\rho \tilde{C}_\alpha^{na}(\rho)$, and the factor $\tilde{C}_{\alpha,\max}^{na} - C_\alpha^m$ was introduced for normalizing $\tilde{Q}_\alpha(\rho)$. For two-qubit states, we

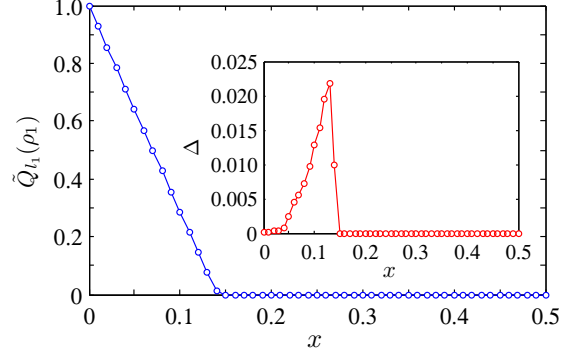


FIG. 4: The x dependence of $\tilde{Q}_{l_1}(\rho_1)$. Here, we choose $x \in [0, 0.5]$ as $\tilde{Q}_{l_1}(\rho_1)$ is symmetric with respect to $x = 0.5$ for ρ_1 . The inset shows the x dependence of $\Delta = \tilde{Q}_{l_1}(\rho_1) - Q_{l_1}(\rho_1)$.

have $\tilde{C}_{\alpha,\max}^{na} = 3$ ($\alpha = l_1$ or re), which are obtained for the Bell states $|\Phi^\pm\rangle = (|00\rangle \pm |11\rangle)/\sqrt{2}$ and $|\Psi^\pm\rangle = (|01\rangle \pm |10\rangle)/\sqrt{2}$. Moreover, we have used the fact that C_α^m cannot be increased by any unitary transformation in the above definition.

Of course, one may propose to define the NAQC-based correlation measure [denoted $Q_{l_1}(\rho)$] by replacing $\tilde{C}_\alpha^{na}(\rho)$ in Eq. (19) with $C_\alpha^{na}(\rho)$. But if so, $Q_{l_1}(\rho)$ will not be locally unitary invariant, thus makes it violates the widely accepted property of a quantum correlation measure (e.g., Bell nonlocality, steerability, entanglement, and quantum discord) which should be locally unitary invariant.

As an example, we calculated numerically the NAQC-based correlation measure of the following state

$$\rho_1 = x|\Phi^+\rangle\langle\Phi^+| + (1-x)|\Psi^-\rangle\langle\Psi^-|, \quad x \in [0, 1], \quad (20)$$

for which $\tilde{Q}_{l_1}(\rho_1)$ is symmetric with respect to $x = 0.5$. As was showed in Fig. 4, $\tilde{Q}_{l_1}(\rho_1) > Q_{l_1}(\rho_1)$ in the region of $0 \leq x \leq 0.141$. In particular, we have $\tilde{Q}_{l_1}(\rho_1) > 0$ and $Q_{l_1}(\rho_1) = 0$ when $0.138 \leq x \leq 0.141$, that is, \tilde{Q}_{l_1} captures a wider region of NAQC states than Q_{l_1} .

ACKNOWLEDGMENTS

This work was supported by National Natural Science Foundation of China (Grants No. 11675129, No. 91536108, and No. 11774406), National Key R & D Program of China (Grants No. 2016YFA0302104 and No. 2016YFA0300600), the New Star Project of Science and Technology of Shaanxi Province (Grant No. 2016KJXX-27), the Strategic Priority Research Program of Chinese Academy of Sciences (Grant No. XDB28000000), and the New Star Team of XUPT.

Appendix A: Constraints imposed on the parameters of $\tilde{\rho}$

At the edge AB of \mathcal{T} , we have $v_1 = v_3$ and $v_2 = -1$. Then the positive semidefiniteness of $\tilde{\rho}$ requires

$$\begin{aligned} \tilde{\rho}_{11}\tilde{\rho}_{44} - |\tilde{\rho}_{14}|^2 &= -(r_3 + s_3)^2 \geq 0, \\ \tilde{\rho}_{22}\tilde{\rho}_{33} - |\tilde{\rho}_{23}|^2 &= -(r_3 - s_3)^2 \geq 0, \end{aligned} \quad (A1)$$

from which one can obtain $r_3 = s_3 = 0$.

Moreover, all the i th-order principal minors of $\tilde{\rho}$ should be nonnegative. Under the constraint $r_3 = s_3 = 0$ obtained above, the second- and third-order leading principal minors $D_{2,3}$ and the principal minor Δ_3 (determinant of the matrix obtained by removing from $\tilde{\rho}$ its third row and third column) are

$$\begin{aligned} D_2 &= 1 - v_1^2 - s_1^2 - s_2^2, \\ D_3 &= (v_1 - 1)[(r_1 + s_1)^2 + (r_2 + s_2)^2], \\ \Delta_3 &= -(v_1 + 1)[(r_1 - s_1)^2 + (r_2 + s_2)^2], \end{aligned} \quad (\text{A2})$$

which, together with Eq. (A1), yields the following requirements

$$r_{1,3} = s_{1,3} = 0, \quad r_2 = -s_2, \quad s_2^2 \leq 1 - v_1^2. \quad (\text{A3})$$

Similarly, one can obtain constraints imposed on the parameters of $\tilde{\rho}$ at the other edges of \mathcal{T} . They are

$$\begin{aligned} AC: & r_{2,3} = s_{2,3} = 0, \quad r_1 = -s_1, \quad s_1^2 \leq 1 - v_3^2, \\ AD: & r_{1,2} = s_{1,2} = 0, \quad r_3 = -s_3, \quad s_3^2 \leq 1 - v_2^2, \\ CD: & r_{1,3} = s_{1,3} = 0, \quad r_2 = s_2, \quad s_2^2 \leq 1 - v_1^2, \\ BD: & r_{2,3} = s_{2,3} = 0, \quad r_1 = s_1, \quad s_1^2 \leq 1 - v_3^2, \\ BC: & r_{1,2} = s_{1,2} = 0, \quad r_3 = s_3, \quad s_3^2 \leq 1 - v_2^2. \end{aligned} \quad (\text{A4})$$

For $\tilde{\rho}$ associated with \vec{v} at the line AO' , we have $v_{1,2} = a_0$ and $v_3 = 1 + 2a_0$ ($-1 \leq a_0 \leq 0$), then a similar derivation gives

$$\begin{aligned} r_{1,2} &= -s_{1,2}, \quad r_3 = s_3 \in [-1 - a_0, 1 + a_0], \\ |s_1| &\leq \min\left\{1 + \frac{1}{2}a_0, \frac{1}{2}(1 - a_0)\right\}, \\ s_1^2 + s_2^2 &\leq -4a_0(1 + a_0). \end{aligned} \quad (\text{A5})$$

Appendix B: Intersection of two surfaces

Due to the symmetry, one only needs to consider the intersections of the level surface \mathcal{S}_A described by Eq. (9) and the facet of \mathcal{P} with the vertices (v_0, v_0, v_0) , $(-1, \gamma, \gamma)$, $(\gamma, -1, \gamma)$. The plane equation for this facet is

$$av_1 + av_2 + cv_3 + 1 = 0, \quad (\text{B1})$$

where

$$a = \frac{v_0 - \gamma}{v_0(1 + \gamma)}, \quad c = -\frac{1}{v_0} - 2a. \quad (\text{B2})$$

Without loss of generality, we fix $(i, j, k) = (1, 2, 3)$ in Eq. (9). Then by plugging $v_1 = \sin \theta$ and $v_2 = \cos \theta$ into Eq. (B1), we obtain

$$v_3 = \frac{(v_0 - \gamma)(\sin \theta + \cos \theta) + v_0(1 + \gamma)}{1 + 2v_0 - \gamma}, \quad (\text{B3})$$

and for given v_0 and γ , one can check whether there are intersections for the two surfaces by checking whether v_3 obtained in Eq. (B3) belongs to the region $[\max\{\sin \theta, \cos \theta\}, 1 + \sin \theta +$

$\cos \theta]$. If there exists such v_3 , then there are intersection of \mathcal{S}_A and \mathcal{P} . Otherwise, \mathcal{S}_A is totally inside or outside of \mathcal{P} .

One can also determine whether there are intersections of \mathcal{S}_A and \mathcal{P} by plugging Eq. (9) into Eq. (B1), and checking the resulting $\text{sgn}(av_1 + av_2 + cv_3 + 1)$. The surface \mathcal{S}_A is inside \mathcal{P} if it is always nonnegative. In fact, here one only needs to check the points at the boundary of \mathcal{S}_A .

Based on the above methods, it is direct to show that when $v_0 = -1/\sqrt{2}$ and $|\gamma| < \sqrt{2} - 1$, the level surface \mathcal{S}_A is always inside \mathcal{P} . When $v_0 \leq -0.7082$ and $\gamma = b_0$, the boundary of \mathcal{S}_A inside the tetrahedron \mathcal{T} is also inside the polyhedron \mathcal{P} .

Similarly, by substituting $v_1 = \sin \theta$, $v_2 = \cos \theta$, and $v_3 = 1 + \sin \theta + \cos \theta$ into the equation of the straight line FG (see Fig. 2), one can obtain

$$(1 + a_0) \sin \theta + (b_0 - a_0) \cos \theta = a_0(1 + b_0). \quad (\text{B4})$$

For given a_0 and b_0 , if there are solutions for Eq. (B4) in the region of $\theta \in [\pi, 1.5\pi]$, there are intersections of FG and the boundary of \mathcal{S}_A described by $v_3 = 1 + \sin \theta + \cos \theta$. In this way, one can check that when $b_0 \approx -0.3813$ and $a_0 \leq -0.7082$, there are no intersections of FG and the boundary of \mathcal{S}_A .

Appendix C: NAQC of general two-qubit states

Suppose $U_{AB} = U_A \otimes U_B$ gives the map $\vec{r} \mapsto \vec{x}$, $\vec{s} \mapsto \vec{y}$, and $\vec{v} \mapsto T = (t_{ij})$, then the transformed state of $\tilde{\rho}$ is given by

$$\rho = \frac{1}{4} \left(I_4 + \vec{x} \cdot \vec{\sigma} \otimes I_2 + I_2 \otimes \vec{y} \cdot \vec{\sigma} + \sum_{i,j=1}^3 t_{ij} \sigma_i \otimes \sigma_j \right), \quad (\text{C1})$$

and we have the following equalities

$$|\vec{r}| = |\vec{x}|, \quad |\vec{s}| = |\vec{y}|, \quad |\vec{v}|^2 = \sum_{ij} t_{ij}^2. \quad (\text{C2})$$

By further using the mean inequality and the analytical solution of $C_l^{na}(\rho)$ given in Ref. [39], we obtain

$$\begin{aligned} C_l^{na}(U_{AB}\tilde{\rho}U_{AB}^\dagger) &\leq \sqrt{\frac{3}{2}(|\vec{v}|^2 + \sum_i t_{ii}^2) + 6|\vec{s}|^2}, \\ &\leq \sqrt{3|\vec{v}|^2 + 6|\vec{s}|^2}, \end{aligned} \quad (\text{C3})$$

hence for the class of $\tilde{\rho}$ with $|\vec{v}|^2 + 2|\vec{s}|^2 \leq 2$, we are sure that $C_l^{na}(U_{AB}\tilde{\rho}U_{AB}^\dagger) \leq \sqrt{6}$. This class of $\tilde{\rho}$ includes (but not limited to) all $\tilde{\rho}$ with $|\vec{s}|^2 \leq 1/4$ as we have $|\vec{v}|^2 \leq 3/2$ for $M(\tilde{\rho}) \leq 1$.

For the relative entropy of NAQC, due to its complexity, we consider only the case of ρ_{Bell} , for which we have

$$\begin{aligned} C_{re}^{na}(U_{AB}\rho_{\text{Bell}}U_{AB}^\dagger) &= \frac{1}{2} \sum_{i \neq j} H\left(\frac{1 + t_{ij}}{2}\right) \\ &\quad - \sum_i H\left(\frac{1 + \sqrt{\sum_j t_{ij}^2}}{2}\right), \end{aligned} \quad (\text{C4})$$

then by using $|\vec{v}|^2 \leq 3/2$ when $M(\tilde{\rho}) \leq 1$, one can show that the maximum of the right-hand side of Eq. (C4) is of about 1.1974, which is achieved when $T = \text{diag}\{v_0, v_0, v_0\}$, with $v_0 = -1/\sqrt{2}$. Hence $C_{re}^{na}(U_{AB}\rho_{\text{Bell}}U_{AB}^\dagger) < C_{re}^m$ for this class of $\tilde{\rho}$.

For general $\tilde{\rho}$ inside the level surface \mathcal{S} , it is hard even to give a numerical simulation as the derivation of the constraints imposed on \vec{r} and \vec{s} is also a difficult task. But if the number of the involved parameters can be reduced, a numerical verification may also be possible. Several examples where such a verification can be performed are as follows:

(1) For the class of $\tilde{\rho}$ at the vertex $(0, -1, 0)$ of \mathcal{O} (the cases for the other vertices of \mathcal{O} are similar), we have $r_{1,3} = s_{1,3} = 0$ and $r_2 = -s_2$, i.e., there is only one variable. We performed numerical calculation with 10^7 equally distributed local unitaries generated according to the Haar measure [44, 45], and found that the maximal $C_{l_1}^{na}$ and C_{re}^{na} achievable by optimizing over $U_A \otimes U_B$ increase with the increase of $|s_2|$. When $|s_2| = 1$, their maximal values are $\sqrt{6}$ and C_{re}^m , respectively. The corresponding optimal $U_{AB}\tilde{\rho}U_{AB}^\dagger$ is of the form of Eq. (C1), with

$$\vec{x} = -\vec{y} = \left(\pm \frac{1}{\sqrt{3}}, \pm \frac{1}{\sqrt{3}}, \pm \frac{1}{\sqrt{3}} \right), \quad t_{ij} = -\frac{1}{3} \quad (\forall i, j). \quad (\text{C5})$$

(2) For the class of $\tilde{\rho}$ associated with $v_{1,2,3} = -1/\sqrt{2}$ (the cases for $v_i = v_j = -v_k = 1/\sqrt{2}$ are similar), the parameter regions can be reduced via $r_3^2 + s_3^2 \leq 1 - v_1^2$ and $|r_{1,3} \pm s_{1,3}| \leq 1 \pm v_1$. The numerical results show that $C_{\alpha}^{na}(U_{AB}\tilde{\rho}U_{AB}^\dagger)$ is still smaller than C_{α}^m ($\alpha = l_1$ or re). Specifically, when $w_{0,1} = \pm 1$, s_1 and r_1 take the values of Eq. (13), the NAQC of $\tilde{\rho}$ cannot be enhanced by U_{AB} , i.e., $C_{l_1}^{na}(\tilde{\rho}) \simeq 2.4405$ and $C_{re}^{na}(\tilde{\rho}) \simeq 2.0026$ are already the maximum values.

(3) For the class of $\tilde{\rho}$ with $v_{1,2} = -1/\sqrt{2}$ and $v_3 = 1 - \sqrt{2}$ [an intersection of AO' and the curve of $M(\tilde{\rho}) = 1$], one can obtain $|\vec{s}|^2 \leq \sqrt{2} - 1$ by using Eq. (A5). Hence $|\vec{v}|^2 + 2|\vec{s}|^2 < 2$, and $C_{l_1}^{na}(U_{AB}\tilde{\rho}U_{AB}^\dagger)$ cannot exceed $\sqrt{6}$ due to Eq. (C3). For NAQC characterized by the relative entropy, we performed numerical calculation with 10^3 equally distributed $\tilde{\rho}$ of this class, while every $\tilde{\rho}$ is further optimized over 10^7 equally distributed local unitaries. From these calculation we still have not found the case for which $C_{re}^{na}(U_{AB}\tilde{\rho}U_{AB}^\dagger) > C_{re}^m$.

-
- [1] M. A. Nielsen and I. L. Chuang, *Quantum Computation and Quantum Information* (Cambridge University Press, Cambridge, UK, 2000).
- [2] M. Genovese, Phys. Rep. **413**, 319 (2005).
- [3] R. Horodecki, P. Horodecki, M. Horodecki, and K. Horodecki, Rev. Mod. Phys. **81**, 865 (2009).
- [4] D. Cavalcanti and P. Skrzypczyk, Rep. Prog. Phys. **80**, 024001 (2017).
- [5] K. Modi, A. Brodutch, H. Cable, T. Paterek, and V. Vedral, Rev. Mod. Phys. **84**, 1655 (2012).
- [6] H. M. Wiseman, S. J. Jones, and A. C. Doherty, Phys. Rev. Lett. **98**, 140402 (2007).
- [7] S. J. Jones, H. M. Wiseman, and A. C. Doherty, Phys. Rev. A **76**, 052116 (2007).
- [8] G. Adesso, T. R. Bromley, and M. Cianciaruso, J. Phys. A **49**, 473001 (2016).
- [9] A. C. S. Costa and R. M. Angelo, Phys. Rev. A **93**, 020103 (2016).
- [10] A. C. S. Costa, M. W. Beims, and R. M. Angelo, Physica A **461**, 469 (2016).
- [11] V. S. Gomes and R. M. Angelo, Phys. Rev. A **97**, 012123 (2018).
- [12] A. Streltsov, G. Adesso, and M. B. Plenio, Rev. Mod. Phys. **89**, 041003 (2017).
- [13] M. L. Hu, X. Hu, J. C. Wang, Y. Peng, Y. R. Zhang, and H. Fan, Phys. Rep., <https://doi.org/10.1016/j.physrep.2018.07.004>.
- [14] T. Baumgratz, M. Cramer, and M. B. Plenio, Phys. Rev. Lett. **113**, 140401 (2014).
- [15] C. Napoli, T. R. Bromley, M. Cianciaruso, M. Piani, N. Johnston, and G. Adesso, Phys. Rev. Lett. **116**, 150502 (2016).
- [16] M. Piani, M. Cianciaruso, T. R. Bromley, C. Napoli, N. Johnston, and G. Adesso, Phys. Rev. A **93**, 042107 (2016).
- [17] C. S. Yu, Phys. Rev. A **95**, 042337 (2017).
- [18] X. Yuan, H. Zhou, Z. Cao, and X. Ma, Phys. Rev. A **92**, 022124 (2015).
- [19] A. Winter and D. Yang, Phys. Rev. Lett. **116**, 120404 (2016).
- [20] X. Qi, T. Gao, and F. Yan, J. Phys. A **50**, 285301 (2017).
- [21] K. Bu, U. Singh, S. M. Fei, A. K. Pati, and J. Wu, Phys. Rev. Lett. **119**, 150405 (2017).
- [22] E. Chitambar, A. Streltsov, S. Rana, M. N. Bera, G. Adesso, and M. Lewenstein, Phys. Rev. Lett. **116**, 070402 (2016).
- [23] A. Streltsov, E. Chitambar, S. Rana, M. N. Bera, A. Winter, and M. Lewenstein, Phys. Rev. Lett. **116**, 240405 (2016).
- [24] A. Mani and V. Karimipour, Phys. Rev. A **92**, 032331 (2015).
- [25] X. Hu, A. Milne, B. Zhang, and H. Fan, Sci. Rep. **6**, 19365 (2016).
- [26] Y. Yao, G. H. Dong, L. Ge, M. Li, and C. P. Sun, Phys. Rev. A **94**, 062339 (2016).
- [27] M. L. Hu, S. Q. Shen, and H. Fan, Phys. Rev. A **96**, 052309 (2017).
- [28] T. R. Bromley, M. Cianciaruso, and G. Adesso, Phys. Rev. Lett. **114**, 210401 (2015).
- [29] M. L. Hu and H. Fan, Sci. Rep. **6**, 29260 (2016).
- [30] M. N. Bera, T. Qureshi, M. A. Siddiqui, and A. K. Pati, Phys. Rev. A **92**, 012118 (2015).
- [31] E. Bagan, J. A. Bergou, S. S. Cottrell, and M. Hillery, Phys. Rev. Lett. **116**, 160406 (2016).
- [32] S. Cheng and M. J. W. Hall, Phys. Rev. A **92**, 042101 (2015).
- [33] U. Singh, M. N. Bera, H. S. Dhar, and A. K. Pati, Phys. Rev. A **91**, 052115 (2015).
- [34] A. Streltsov, U. Singh, H. S. Dhar, M. N. Bera, and G. Adesso, Phys. Rev. Lett. **115**, 020403 (2015).
- [35] Y. Yao, X. Xiao, L. Ge, and C. P. Sun, Phys. Rev. A **92**, 022112 (2015).
- [36] J. Ma, B. Yadin, D. Girolami, V. Vedral, and M. Gu, Phys. Rev. Lett. **116**, 160407 (2016).
- [37] M. L. Hu and H. Fan, Phys. Rev. A **95**, 052106 (2017).
- [38] X. Hu and H. Fan, Sci. Rep. **6**, 34380 (2016).
- [39] D. Mondal, T. Pramanik, and A. K. Pati, Phys. Rev. A **95**, 010301 (2017).
- [40] J. F. Clauser, M. A. Horne, A. Shimony, and R. A. Holt, Phys. Rev. Lett. **23**, 880 (1969).

- [41] R. Horodecki, P. Horodecki, and M. Horodecki, Phys. Lett. A **200**, 340 (1995).
- [42] R. Horodecki and M. Horodecki, Phys. Rev. A **54**, 1838 (1996).
- [43] R. Horodecki, M. Horodecki, and P. Horodecki, Phys. Lett. A **222**, 21 (1996).
- [44] F. Mezzadri, Not. Am. Math. Soc. **54**, 592 (2007).
- [45] M. L. Mehta, *Random Matrices* (Elsevier, Amsterdam, 2004).